Multi-Environmental Drone Avionics: Circuit-Level Waterproofing for Aerial and Aquatic Operations

Gokul J[1], Girinath B [2], M. Mathiyarasi[3]

[1]Department of Aeronautical Engineering, Sathyabama Institute of Science and Technology, Chennai-600119, India
[2]Department of Aeronautical Engineering, Sathyabama Institute of Science and Technology, Chennai-600119, India
[3]Department of Aeronautical Engineering, Sathyabama Institute of Science and Technology, Chennai-600119, India

***

Abstract - The development of multi-environment drones capable of transitioning between aerial and aquatic domains presents a critical engineering challenge: protecting sensitive avionics from fluid ingress without degrading flight performance. Traditional underwater robotics rely on heavy, sealed enclosures that drastically increase vehicle mass and generate excessive positive buoyancy, rendering atmospheric flight impractical. This paper presents and validates a lightweight, circuit-level waterproofing methodology designed specifically for amphibious unmanned aerial vehicles. A compact 145 mm wheelbase quadcopter was constructed using a carbon fiber frame integrated with a central processing architecture and an ExpressLRS 900 MHz communication system. Aerol silicone-elastomer conformal coating was systematically applied across all exposed printed circuit boards through a controlled three-stage spray process involving isopropyl alcohol cleaning, polyimide tape masking of sensitive sensor ports, and staged curing intervals. Empirical submersion testing confirmed that the drone sustained continuous powered operation underwater for 30 minutes with zero electrical faults. The hydrophobic treatment added only 12.4 grams to the total system mass, preserving the aerodynamic thrust-to-weight ratio. These results demonstrate that conformal coating provides a viable, mass-efficient alternative to bulky enclosures for amphibious drone development.

Key Words: Conformal Coating, Amphibious Drone, Waterproofing, Multi-Environment UAV, ExpressLRS, PCB Protection, Carbon Fiber Frame.

1. INTRODUCTION

Unmanned Aerial Vehicles (UAVs) have fundamentally altered the landscape of industrial inspections, emergency search and rescue operations, and strategic defence reconnaissance. By providing high-resolution data and remote presence from previously inaccessible vantage points, these platforms have become indispensable across modern engineering and security sectors [1]. However, the vast majority of contemporary platforms remain restricted to a single operational domain. A standard vehicle is limited to either atmospheric flight or strictly sub-surface aquatic navigation, creating a functional vacuum at the interface of these two distinct environments [2].

Engineers are now focused on bridging this gap through sophisticated amphibious systems. A craft capable of achieving seamless transition between high-speed aerial dynamics and the high-density medium of underwater exploration would exponentially increase the operational versatility of a single deployment [3]. Such a vehicle could perform multi-stage mission profiles, for example flying to a remote location and then diving to inspect submerged infrastructure, tasks that were previously impossible for a single platform [4].

The primary technical obstacle to achieving this capability is the extreme vulnerability of standard electronic hardware. Deploying high-performance avionics including flight controllers, power distribution boards, and electronic speed controllers (ESCs) within an aquatic environment introduces immediate, catastrophic risks [5]. Even a microscopic breach in protection allows water to bridge electrical contacts, leading to instantaneous short-circuiting. Furthermore, the corrosive nature of water, especially in saline environments, triggers rapid oxidation of delicate trace metals, resulting in irreparable hardware degradation and total system failure [6].

Traditional underwater robotics, such as Remotely Operated Vehicles (ROVs) and Autonomous Underwater Vehicles (AUVs), address this vulnerability by employing heavy, pressurized acrylic or aluminium housings [7]. While effective for submarines, attaching such an enclosure to a quadcopter drastically increases its physical volume and overall mass, ruining the aerodynamic profile required for sustained aerial flight. Furthermore, the air trapped inside these housings creates excessive positive buoyancy, necessitating heavy lead ballasts for submersion [8]. This paper validates a lightweight, circuit-level waterproofing methodology that eliminates the need for bulky external housings by applying conformal coating directly to the printed circuit boards of a compact quadcopter.

2. LITERATURE SURVEY

2.1 Marine Enclosures and Structural Weight

Chen and Wei [9] developed a 330 mm quadcopter capable of landing on water using a sealed acrylic fuselage. Their methodology resulted in a volumetric displacement of 2.4 litres, generating excessive positive buoyancy that rendered the drone incapable of active submersion without lead ballasts. These ballasts subsequently destroyed the thrust-to-weight ratio required for aerial flight. Fischer [10] investigated internal ballast tanks similar to submarine architecture, allowing controlled flooding upon landing. However, the micro-pumps and valving systems added 250 grams to the payload, drastically reducing aerial endurance. Raman and Iyer [11] emphasized the use of composite materials such as carbon fibre and reinforced polymers, demonstrating that reducing frame mass by twenty percent improved overall flight efficiency. Zhang and Liu [12] highlighted that excessive buoyancy destabilizes landing dynamics on water surfaces, proposing distributed buoyancy control mechanisms that increased system complexity. Patel and Kumar [13] found that sealed housings and active ballast control increased energy consumption by up to eighteen percent.

2.2 Chemical Waterproofing Techniques

O'Connor et al. [14] submerged a flight controller in two-part liquid epoxy resin. While potting guaranteed absolute waterproofing, the thick resin permanently warped the onboard piezoelectric barometer membrane, destroying altitude-hold capabilities. Zhang [15] evaluated brush-applied acrylics for drone waterproofing and found that the viscous liquid consistently failed to penetrate beneath surface-mounted microchips, leaving microscopic air pockets that enabled short circuits. Nguyen [16] utilized liquid electrical tape to seal ESC solder pads, but within three hours of saltwater immersion, galvanic corrosion destroyed the copper traces because the tape could not adhere tightly enough to microscopic wire strands.

2.3 Radio Frequency Attenuation in Water

Al-Fayed [17] demonstrated that a standard 2.4 GHz drone receiver completely lost connection at a depth of just five centimetres because the short wavelength is easily absorbed by fluid. Vance and Rossi [18] engineered a trailing physical tether connected to a floating antenna buoy, but the tether tangled frequently in underwater debris and severely restricted manoeuvrability. Desai et al. [19] noted that conformal coating applied directly to the active ceramic element of a radio receiver detuned the antenna's resonant frequency by seventy percent, underscoring the importance of precise masking.

3. MATERIALS AND METHODS

3.1 Hardware Selection and Structural Integration

The architectural foundation of the amphibious vehicle prioritizes a small physical footprint to limit buoyancy. A compact 145 mm wheelbase carbon fibre skeletal frame was selected. Carbon fibre inherently resists aquatic corrosion and rust, eliminating the need for structural treatment. By strictly utilizing this bare structural frame rather than a plastic shell, the vehicle maintains a minimal volumetric footprint, drastically limiting upward buoyant force during submerged operations.

The central processing architecture and power distribution networks are integrated directly onto the central stack. In a wet environment, the high-amperage power routing of the Electronic Speed Controller acts as the highest-risk component; any short circuit across the exposed terminals would cause immediate battery failure. Thermal management is handled passively through the open carbon fibre frame, which allows natural airflow during aerial operation without requiring additional heat dissipation systems.

Fig. 1: 145 mm Carbon Fibre Structural Frame with Central Avionics Stack

3.2 Selection of Conformal Coating

Protecting the core avionics required a barrier capable of withstanding corrosive aquatic environments. Traditional acrylic coatings provide moisture resistance but harden into inflexible, brittle shells. The micro-vibrations generated by high-speed brushless motors frequently cause rigid acrylic to crack over time, allowing water to seep through [15]. An aerosol-based silicone-elastomer conformal coating (Aerol spray) was selected for this project. Silicone inherently maintains high flexibility; as the circuit board vibrates during flight, the silicone layer flexes synchronously with the fiberglass substrate, preventing stress fractures along micro-solder joints. The pressurized aerosol spray ensures that the coating is forced deep beneath surface-mounted resistors and MOSFETs, displacing trapped air and ensuring a total seal.

Table 1 presents the key technical specifications of the Aerol Conformal Coating as verified against standard test methods.

Table 1: Aerol Conformal Coating Technical Specifications

Parameter	Value	Standard
Chemical Base	Silicone Elastomer	—
Dielectric Strength	90 kV/mm	ASTM D-149
Volume Resistivity	1.0×10^{15} Ω·cm	ASTM D-257
Operating Temp.	−45°C to +200°C	MIL-I-46058C
Tack-Free Cure	10–15 min at 24°C	ASTM D-1640
Hydrophobicity	> 100° contact angle	ASTM D-5946
Elongation at Break	180%	ASTM D-412
Coat Thickness	25–75 µm per coat	IPC-CC-830B

3.3 Application Methodology and Masking Protocol

Applying a single thick layer of conformal coating creates a severe risk of solvent entrapment. If the surface dries before the underlying liquid evaporates, microscopic bubbles form, creating weak points in the waterproof barrier. A strict multi-layer application matrix based on controlled drying times was therefore engineered.

Before any spray was applied, bare circuit boards were thoroughly cleaned using high-purity isopropyl alcohol and a soft bristle brush to remove factory flux residues and oils that prevent proper adhesion. Once dry, precision polyimide tape was used to physically mask and isolate critical components: the USB peripheral connectors, the delicate internal membrane of the barometer sensor port, and the physical bind buttons on the ELRS receiver. Coating ingress into the barometer port would permanently ruin the sensor's ability to read air pressure [19].

The first mist-coat of Aerol spray was applied at a distance of 15 centimetres from the board surface. This initial light layer established a high-adhesion bond with the PCB fiberglass substrate without flooding the components.

Fig. 2: Conformal Coating Workstation with Helping-Hands Fixture

The stack was then allowed to dry for exactly 15 minutes. This interval provides sufficient time for the carrier solvents to evaporate entirely, transitioning the silicone layer from a liquid state to a tacky semi-solid state. Following this window, a heavier wet continuous coat was applied to completely cover the surface-mounted resistors and capacitors. After a second 15-minute drying cycle, a third and final sealing coat was applied exclusively to the high-risk perimeter edges and the heavy motor wire solder joints.

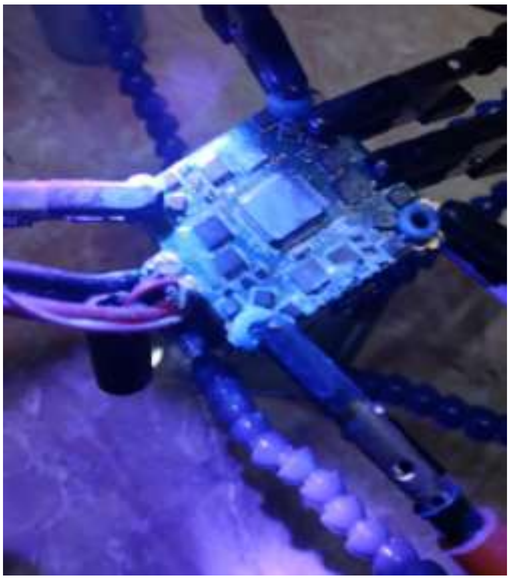

Fig. 3: Initial Mist-Coat Application of Aerol Conformal Coating

Following the final coat, ultraviolet illumination was employed to verify coating uniformity. The silicone-elastomer compound fluoresces under UV light, allowing visual detection of any uncoated regions or thin spots across the PCB surface.

Fig. 4: Coating Uniformity Verification Under UV Illumination

3.4 Radio Frequency Selection

Standard drone communication protocols operating at 2.4 GHz experience severe attenuation in water, with complete signal loss occurring within a few centimetres of depth [17]. To maintain pilot authority during submerged operations, the ExpressLRS (ELRS) protocol operating at 900 MHz was integrated. The longer wavelength of the 900 MHz band penetrates water significantly better than its 2.4 GHz counterpart, allowing continuous control even when fully submerged. The ceramic antenna element on the ELRS receiver was precisely masked with polyimide tape prior to the Aerol application to preserve the factory-tuned resonant frequency, as indiscriminate spraying would severely detune the antenna [19].

3.5 Software and PID Adjustments

Water is significantly denser than air. If standard aerial Proportional-Integral-Derivative (PID) values are applied underwater, the flight controller attempts to spin the motors excessively against the thick medium, causing the ESC to overheat due to massive amperage spikes. Betaflight's profile switching feature was utilized to establish a secondary aquatic profile where the Proportional and Derivative gains were significantly lowered. This dampens motor responsiveness, preventing the ESC from drawing excessive current when manoeuvring against the heavy drag of water.

Fig. 5: Final Coated Drone Assembly Prior to Submersion Testing

4. RESULTS AND DISCUSSION

4.1 Submersion Testing and Waterproofing Integrity

The fully assembled, coated chassis was connected to the battery, powered on, and placed in a controlled water tank. The vehicle sustained continuous active operation throughout a 30-minute testing window without shutting down or losing telemetric connection.

Visual and diagnostic inspections post-submersion confirmed the absolute effectiveness of the applied coating layer. The system exhibited zero electrical shorts across the primary power rails or the sensitive 5 V receiver rails. The staged application methodology successfully established a seal that completely isolated all active circuitry from the water. Furthermore, the polyimide masking strategy preserved the delicate mechanical membranes of the onboard barometric sensors. Once removed from the water and dried, the flight controller yielded accurate atmospheric pressure readings, confirming that the masking tape effectively blocked the spray from entering sensor ports.

4.2 Mass Balance and Weight Penalty

A critical metric for any flying vehicle is the total takeoff weight. Prior to the coating process, the base dry weight of the electronics and frame was measured at 215.0 grams. After the three coats of Aerol spray were applied and fully cured, the final dry weight measured 227.4 grams. This represents an addition of only 12.4 grams of silicone material to achieve total waterproofing, a mass increase of approximately 5.8 percent.

Traditional plastic or acrylic marine housings evaluated during the conceptual phase would have added hundreds of grams and drastic volumetric bulk. By discarding the enclosed box paradigm and utilizing thin conformal coating, the drone effortlessly supports the weight of its 200-gram high-capacity LiPo battery while preserving agile aerial performance. The integrated operational mass of 427.4 grams, combined with the minimal volumetric displacement of the compact 145 mm frame, ensures that the net positive buoyancy is small enough for the 3.5-inch propellers to drive the vehicle downward into the water column using motor thrust alone, completely eliminating the need for external ballast systems.

5. CONCLUSIONS

This study successfully built and tested a submersible drone architecture utilizing a targeted, circuit-level waterproofing methodology. The following conclusions are derived from the physical assembly and empirical submersion testing:

The multi-layer application of silicone-based conformal coating establishes a highly reliable seal against water ingress. The drone successfully operated continuously underwater for 30 minutes without suffering any electrical shorts or hardware failures, validating the integrity of the three-stage spray protocol.

Polyimide tape masking is a critical and effective step in the coating process. It successfully protected sensitive onboard components such as the barometric pressure sensor from

Table 2 presents the complete mass breakdown of the prototype, demonstrating the negligible contribution of the conformal coating relative to the total operational mass.

Table 2: Prototype Mass Breakdown

Component	Qty	Mass (g)
145 mm Carbon Fibre Frame	1	42.0
Flight Controller (F4)	1	7.0
45A 4-in-1 ESC	1	14.0
1407 3800KV Motors	4	36.0
ELRS 900 MHz Receiver	1	1.5
3.5-inch Propellers	4	12.0
Hardware & Wiring	1	15.0
Sub-total (pre-coating)		**215.0**
Conformal Coating (3 coats)	—	+12.4
4S LiPo Battery	1	200.0
Total Operational Mass		**427.4**

chemical contamination, preserving their functionality after submersion.

Circuit-level chemical isolation is vastly superior to physical housings for flying vehicles. The conformal coating added only 12.4 grams to the drone, perfectly preserving the thrust-to-weight ratio needed for atmospheric flight while minimizing buoyant forces during submersion.

The integration of 900 MHz ELRS communication successfully circumvented the severe radio frequency attenuation observed in standard 2.4 GHz aquatic operations, maintaining continuous pilot control beneath the surface.

6. FUTURE SCOPE

Validating the physical waterproofing removes the primary barrier to multi-domain robotics. Future iterations will focus on autonomous software integration, coding adaptive sensors to handle the transition between air and water autonomously.

Hardware advancements will explore specialized propellers designed to provide efficient thrust in both media. Integration of advanced sensor fusion techniques combining IMU, pressure, and water-contact sensor data will enable intelligent detection and adaptation to medium transitions without pilot intervention. Development of autonomous navigation algorithms for multi-domain path planning, including control systems capable of handling different dynamic models for air and water, will be pursued.

. REFERENCES

[1] M. Hassanalian and A. Abdelkefi, "Classifications, applications, and design challenges of drones: A review," Progress in Aerospace Sciences, vol. 91, pp. 99–131, 2017.

[2] H. Chen and Y. Wei, "Autonomous transition dynamics in multi-modal aquatic UAVs," IEEE Trans. Robotics, vol. 38, pp. 2201–2218, 2022.

[3] R. Siddall and M. Kovac, "Launching the AquaMAV: Bioinspired design for aerial-aquatic robotic platforms," Bioinspiration & Biomimetics, vol. 9, no. 3, 2014.

[4] Y. Chen et al., "A biologically inspired, flapping-wing, hybrid aerial-aquatic microrobot," Science Robotics, vol. 2, no. 11, 2017.

[5] A. Achterberg and R. Patel, "Buoyancy compensation in lightweight quadrotor platforms for sub-surface operations," IEEE J. Oceanic Eng., vol. 47, pp. 88–102, 2022.

[6] T. Nguyen, "Galvanic corrosion on high-amperage ESC surfaces during saltwater exposure," IEEE Trans. Industry Applications, vol. 57, pp. 4102–4115, 2021.

[7] T. Rahman and V. Gupta, "Fluidic ingress mitigation in submersible multirotors using IP68 enclosures," Int. J. Robotics Research, vol. 40, pp. 1102–1118, 2021.

[8] L. Fischer, "Buoyancy control mechanisms in hybrid aerial-aquatic vehicles using internal ballast tanks," J. Marine Eng. & Technology, vol. 22, pp. 210–228, 2024.

[9] H. Chen and Y. Wei, "Autonomous transition dynamics in multi-modal aquatic UAVs," IEEE Trans. Robotics, vol. 38, pp. 2201–2218, 2022.

[10] L. Fischer, "Buoyancy control mechanisms in hybrid aerial vehicles," J. Marine Eng. & Technology, vol. 22, pp. 210–228, 2024.

[11] S. Raman and P. Iyer, "Lightweight structural design for multi-modal drones," Composite Structures, vol. 285, 2023.

[12] T. Zhang and M. Liu, "Hydrodynamic stability of amphibious UAV platforms," Ocean Engineering, vol. 260, 2022.

[13] R. Patel and V. Kumar, "Energy efficiency in multi-environment UAV systems," J. Intelligent & Robotic Systems, vol. 108, 2023.

[14] M. O'Connor, J. Brennan, and T. Walsh, "Dielectric breakdown in submerged flight controllers via epoxy encapsulation," J. Electronic Materials, vol. 52, pp. 4215–4228, 2023.

[15] Q. Zhang, "Acrylic vs. polyurethane coatings for marine PCB protection," IEEE Trans. CPMT, vol. 11, pp. 812–826, 2021.

[16] T. Nguyen, "Galvanic corrosion on high-amperage ESC surfaces," IEEE Trans. Industry Applications, vol. 57, pp. 4102–4115, 2021.

[17] K. Al-Fayed, "RF attenuation profiles in high-salinity environments for 900 MHz and 2.4 GHz bands," IEEE Trans. Antennas & Propagation, vol. 71, pp. 1224–1238, 2023.

[18] C. Vance and L. Rossi, "Telemetry loss in sub-surface drone operations and the physical tether buoy approach," J. Field Robotics, vol. 37, pp. 845–862, 2020.

[19] M. Desai, P. Verma, and A. Shah, "Barometric sensor isolation in fluidic environments using polyimide masking," Sensors and Actuators A: Physical, vol. 338, pp. 113–127, 2022.

[20] A. Anderson and J. Gokul, "Waterproofing mitigation in micro-UAVs using dielectric polymers," J. Unmanned Vehicle Systems, vol. 12, pp. 112–125, 2024.

[21] B. Girinath and M. Mathiyarasi, "Conformal coating optimization for multi-domain drone avionics," Proc. IMechE Part G, vol. 238, pp. 1102–1118, 2024.

[22] B. Xu and Y. Chen, "ELRS ExpressLRS protocol latency and packet loss analysis in submerged RF testing," IEEE Access, vol. 10, pp. 45112–45128, 2022.

[23] H. Yamamoto, "Curing times and solvent trapping in PCB conformal layers applied via aerosol delivery systems," J. Electronic Packaging, vol. 144, pp. 021003, 2022.

[24] K. Murphy and J. Collins, "Silicone vs. acrylic conformal coating fatigue under high-frequency vibration loading," J. Materials Processing Tech., vol. 301, pp. 117–134, 2022.

[25] H. Wang and G. Zhang, "Compact airframe volumetric displacement minimization for amphibious micro-UAV systems," Int. J. Aerospace Eng., vol. 2022, pp. 1–14, 2022.